energies

MDPI

Article

Energy Consumption Analysis for Coupling Air Conditioners and Cold Storage Showcase Equipment in a Convenience Store

Kusnandar [1], Indra Permana [1], Weiming Chiang [1], Fujen Wang [2,*] and Changyu Liou [2]

[1] Graduate Institute of Precision Manufacturing, National Chin-Yi University of Technology, Taichung 411, Taiwan; kusnandar11@gmail.com (K.); indra.refrigeration@gmail.com (I.P.); art23022431@gmail.com (W.C.)
[2] Department of Refrigeration, Air Conditioning, and Energy Engineering, National Chin-Yi University of Technology, Taichung 411, Taiwan; lioucyda@gmail.com
* Correspondence: fjwang@ncut.edu.tw; Tel.: +886-922-836-010

Abstract: The energy use intensity (EUI) of convenience stores was substantially higher than that of office buildings and hotels, due to a compact footprint but a high density of equipment yielded a higher EUI. As a result, it is critical to assess and maintain the state of the convenience store in order to obtain a lower EUI and reduce energy consumption. This study utilizes a convenience store to evaluate energy consumption and perform a CFD simulation to see how the environment influences by cold storage showcase (CSS) equipment. On the basis of field testing and on-site web-based monitoring data, a survey of baseline information through data collecting and energy benchmarking data has been provided and extensively examined. According to energy monitoring, the convenience store's highest electricity use is 23,055 kWh in June, and the lowest power consumption is 15,216 kWh in February. The CFD simulation results revealed that the temperature near the CSS can be 3–5 °C lower than in other regions. The temperature nearby return air will be lower as a result of the low-temperature air impacts from CSS. The AC sensor detects that the environment has met the indoor requirements and performs the load reduction operation. After adjusting the AC temperature, it is discovered that the unit is unable to attain the appropriate temperature. Energy consumption can be reduced, resulting in more energy-efficient AC and CSS operations. Furthermore, the CSS's cold air effect might be taken advantage of by raising the AC-2 temperature set point to generate energy savings.

Keywords: convenience store; energy consumption; air conditioner; cold storage; computational fluid dynamics

Citation: Kusnandar; Permana, I.; Chiang, W.; Wang, F.; Liou, C. Energy Consumption Analysis for Coupling Air Conditioners and Cold Storage Showcase Equipment in a Convenience Store. *Energies* **2022**, *15*, 4857. https://doi.org/10.3390/en15134857

Academic Editors: Nazrul Islam, Saleem Anwar Khan, Dibakar Rakshit, Abdullatif A. Gari, Abdus Samad and Amjad Ali Pasha

Received: 20 May 2022
Accepted: 29 June 2022
Published: 2 July 2022

1. Introduction

Residential and commercial buildings have the potential to achieve water and electricity savings of 20 to 30 percent. Statistical data analysis performed in 2016 shows a lot of promise for cost-effective energy reductions in Taiwan. The residential and commercial sectors are responsible for 21.72 percent of Taiwan's energy usage [1]. Taiwan had 10,266 convenience stores as of the end of 2016 [2]. Due to the study field and the major concern of a sustainable environment, energy consumption is has been a frequently emphasized problem. However, due to the complexity of the situation, approaching the optimization of energy use in all facilities is fairly difficult. The use of accessible energy modeling to analyze energy use for whole-building simulations is generally acknowledged to be the most successful approach [3].

Convenience stores require more energy than other types of retailers [4]. The results showed that a convenience store's average annual energy consumption intensity (EUI) was 2346 kWh/m^2/year, which was much greater than that of office buildings and hotels [5]. The EUI benchmark range for educational buildings was found to be

47,628 kWh/m^2/year [6]. The building sector's energy usage is steadily increasing, accounting for around 40% of total world energy consumption. Energy consumption of buildings varies and depends both on their purpose and the year of construction [7]. Cooling and refrigeration systems account for around 17% of global power consumption [8]. For energy consumption analyses, heat load and the ambient temperature are both very significant in determining the cooling energy consumption [9]. Energy usage has an impact on grocery profit margins, which are already low (about 1–2%). Electrical energy usage can range from 700 kWh/m^2 of sales space to over 2000 kWh/m^2 in convenience stores, according to Energy Star Certified Buildings and Plants [10]. Many academics have studied how to increase the performance of HVAC systems in order to efficiently minimize energy consumption [11].

Buildings' energy usage is always a major concern. Regulations and rules are widely used to restrict the energy consumption of buildings in order to accomplish the objective of energy conservation. However, the energy index used to assess energy efficiency did not take into account the hybrid use of hotel facilities for various service objectives. Convenience stores with a couple of air conditioners and cold storage units have been thoroughly explored in this study. Regression data might be gathered in large quantities by field measurements and testing of air velocity and temperature as part of a building energy management system (BEMS) study [12]. Thus, energy management systems (EMS) for HVAC and other equipment save around 14.07 percent and 16.66 percent of energy, respectively [13]. Air conditioners are one of the primary causes of summer electrical load peaks, accounting for over half of all power needs during the hot noon hours in some places where electricity is costly. The wholesale power price is reduced as an incentive for use at off-peak periods when utilities have spare electrical producing capacity due to decreased demand [14]. The uniformly distributed indoor velocity and temperature field can further reduce the energy required for air conditioning and refrigeration [15].

Many applications can benefit from simulation, including airflow (through CFD), comfort, and HVAC system design. CFD analysis on thermal comfort and energy consumption is carried out to simulate variables of indoor airflow [16]. When there was more time for the simulation, the optimization simulation was typically closer to the ideal solution [17]. The design of low-energy and efficient buildings is increasingly reliant on building simulation tools for performance prediction, which are frequently coupled to HVAC system design calculations [18]. The research using CFD has been frequently applied sophisticated integrated for investigating detailed information of flow in general [19]. The current CFD model is a useful tool for evaluating air quality and thermal comfort [20]. Several studies have studied interior air velocities using on-site observations and CFD numerical models [21]. CFD predictions that agreed well with the experiment were generated [22]. CFD simulations, when combined with an experimental database, provide precise predictions of in-door airflow, and temperature parameters were studied [23]. Several investigations of the velocity and temperature field in basic three-dimensional geometry have been conducted using CFD, but without confirming the model with actual data [24]. Furthermore, a CFD model was utilized to analyze the average velocity and temperature in a test room cooled ceiling panel; the findings were confirmed using actual data first, and the velocity fields were explored [25].

Field measurements easily determine the features of indoor air quality in various situations [26]. Field measurements are taken to serve as the foundation for the parameters that will be put up in the CFD simulation. These energy-saving capabilities are linked to enhanced EMS functionalities. Furthermore, because of the demands of many green and energy-efficient building standards and certifications, the building energy model has been widely employed in building design. [27]. Field data collection is used to inform and validate this simulation. Simulations are carried out to test and validate the typical fault of mixing functioning of air conditioners and cold store units within the convenience store, as well as the feasibility of energy-efficient techniques in the convenience store. Despite the fact that extensive research on energy efficiency in convenience stores has been undertaken, the results still require additional information.

In this study, a field investigation was conducted to get actual data to use for the boundary conditions in CFD modeling. Based on the simulation results, it has been discovered that adjusting the temperature can most effectively aid in enhancing the thermal comfort conditions [28]. Field measurements are taken to serve as the foundation for the parameters that will be put up in the CFD simulation. To validate the simulation, the CFD simulation is calibrated with the real conditions in the room. The CFD method was used to find the improvement design to provide a comfortable environment for occupants, and the prospects of energy-efficient ways in the convenience store are explored through simulations.

2. System Description

The investigated convenience store is located in the northern region of Taiwan. The general area is about 145.25 m^2, the length is 15 m, the width is 9.5 m, the ceiling height is 3.5 m, and the mezzanine is about 3 m. The electrical equipment in the store includes two microwave ovens, water boilers, two coffee machines, a tea egg cooker, a hot dog machine, a hot can machine, a steaming machine, and an electric cooker. The AC in the store adopts the direct expansion type air conditioner; the main engine is two 6 RT inverter air conditioners, and the air outlet equipment adopts the embedded type all-around blowing. The indoor air conditioner temperature is set to 26 °C. The indoor lamps and the indoor lamps use T8 lamps. The indoor unit of AC is placed on one table in front of the counter, and the other is above the middle aisle of the central island-type open display cabinet. On the other hand, the CSS equipment has 2 island-type open display cabinets, combination refrigerators, freezer refrigerators, 6-foot open refrigerators, 4-foot horizontal refrigerators, and ice cream machines, as sketched in Figure 1a.

Figure 1b is the floor plan of the supermarket, which is divided into two areas, the business space, and the rear storage room. The beverage refrigerator is in the rear storage room, and there is a glass display door in the direction of the business space on the lower left side of the business space. For the snack placement area, two island-style open display cabinets are placed in front of the middle counter, and hot food heating equipment such as steaming machines and electric cookers are placed in the hot food area on the right. Large-scale machine equipment such as printers and multimedia consoles are in the upper left half of the room. Section A-A′ plane will be used to evaluate the cold feet effect resulting from the CSS equipment that produces cold air. Then, section B-B′ plane will be used to evaluate the temperature variation from the AC-1 and AC-2 at different heights from the floor to the ceiling.

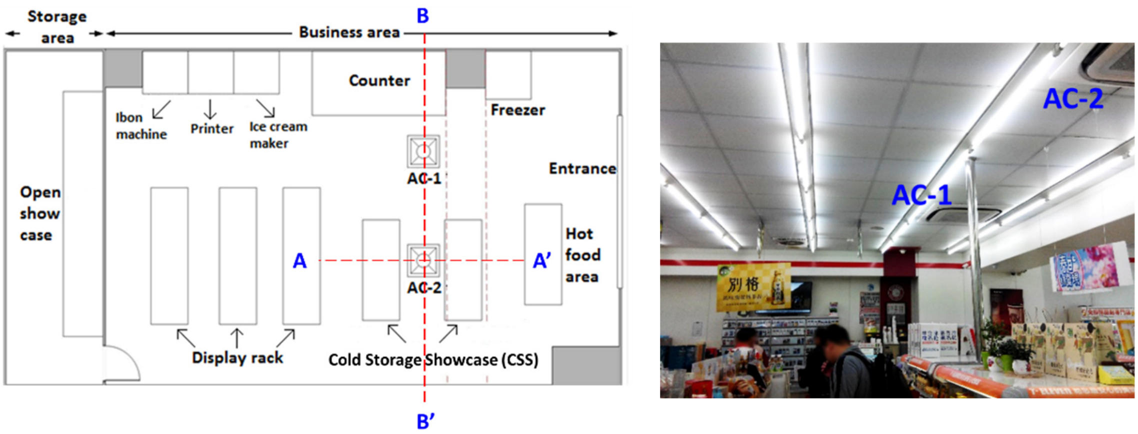

(**a**) (**b**)

Figure 1. Investigated convenience store; (**a**) AC location; (**b**) layout.

3. Field Measurement

Field tests were carried out in order to offer a solid baseline for comparison and to validate the simulation results for performance improvement and energy-saving potential evaluation. A TSI model 8380 was used in this experiment to measure the velocity of each air velocity at AC. Then, using a velocity matrix, determine the air supply velocity. The TSI-8380 sensor captured the AC airflow rate with a 3 percent accuracy. The temperature and relative humidity of a room or location have a significant impact on the things in the room. The temperature in this convenience store is regulated between 22 °C and 28 °C, with a 2 °C tolerance. The temperature and humidity levels in this convenience store were measured with the TSI model 9565P. The power meter model is HIOKI-3169-20/21, having an operating range of 0–600 Vrms 0.5 A–5000 A. Previous studies have looked into wearable devices, temperature sensors, and human motion detectors combined as smart sensors to provide smart AC control. The results reveal that interior temperature can be precisely regulated with errors of less than 0.1 °C [29]. Table 1 depicts the field measuring device used at a convenience store.

Table 1. Apparatus for the field measurement.

Apparatus Model	Item	Operative Range	Accuracy
TSI-8380	Velocity	0.125–12.5 m/s	±3%
	Pressure	Diff ± 3735 pa	±2%
TSI 9565TP	Temperature	−10~60 °C	±0.3 °C
	Humidity	5–95% RH	±3%
HIOKI-3169	Power Meter	0–600 Vrms, 0.5–5000 A	±3%

The demand for data acquisition and electrical loading systems has become apparent in testing power consumption energy devices. A data acquisition system instrumented without modifying and recording airflow and rate temperature was successful in system measurement using Power Data Acquisition System (PDAS). The Internet of Things (IoT) sensing controller is used to measure environmental parameters such as temperature, humidity, carbon dioxide, and other information that can also be obtained by communicating with the subsystem through the 2.4 G wireless module. Due to the large amount of equipment in the supermarket, according to the configuration of the on-site power distribution board, the configuration diagram of the energy consumption monitoring and measurement system is shown in Figure 2. Each device is connected through each multi-channel cloud meter. The information is transmitted to the cloud monitoring transmitter, then transmitted to the cloud database through the network. All equipment information can be displayed on the webpage. At the same time, the loop connection is mainly based on the convenience of construction and on-site space, which can monitor the hourly, daily, and even monthly energy consumption of each energy equipment in the reference building to understand the energy usage density and schedule of each equipment that can use as a reference for the input parameters of the energy simulation model.

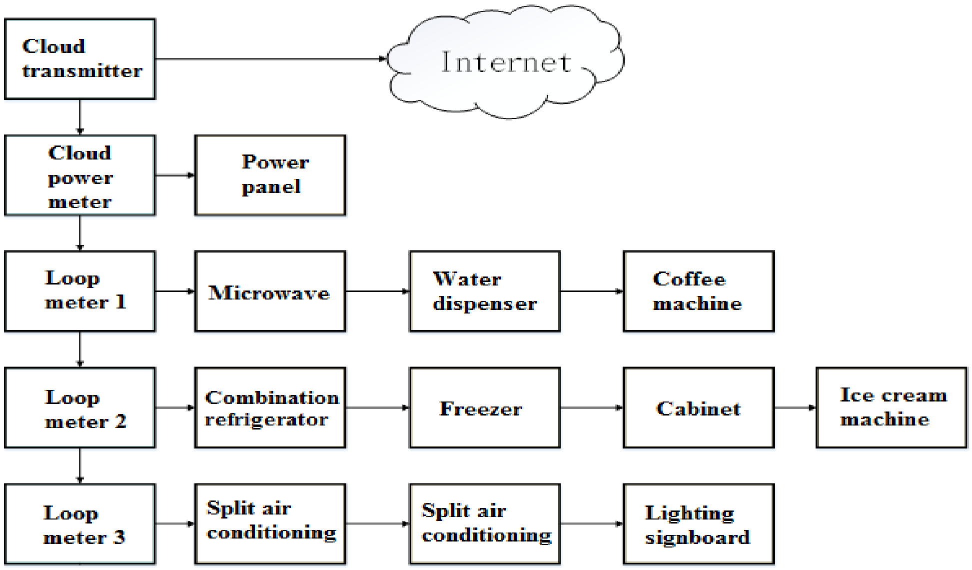

Figure 2. Power data acquisition system (PDAS).

4. Numerical Simulation

Computational Fluid Dynamics (CFD) is a very powerful, useful tool with flexibility, accuracy, and breadth of application for state-of-the-art research and is efficient in parametric studies for airflow and temperature distribution. This study uses ANSYS Fluent code version 2020 R2 [30] to investigate the indoor thermal environment in a convenience store. The layout model from the AutoCAD files was used to construct a 3D model for model establishment using SolidWorks software version 2020. The dimension of the on-site equipment was also measured as the actual condition and place relevant equipment objects to build the full-scale convenience store environment with a length of 15 m, a width of 9.5 m, and a height of 3.5 m, as shown in Figure 3a. The geometry simplifies the complex and multilateral mechanical equipment into regular rectangles of the same size. Although AC and CSS are the focuses of observation, detailed models were established, and two open CSS were arranged according to the site. The CSS is shown in Figure 3b, according to on-site measurements with a length of 2.8 m, a width of 0.6 m, and a height of 1.4 m.

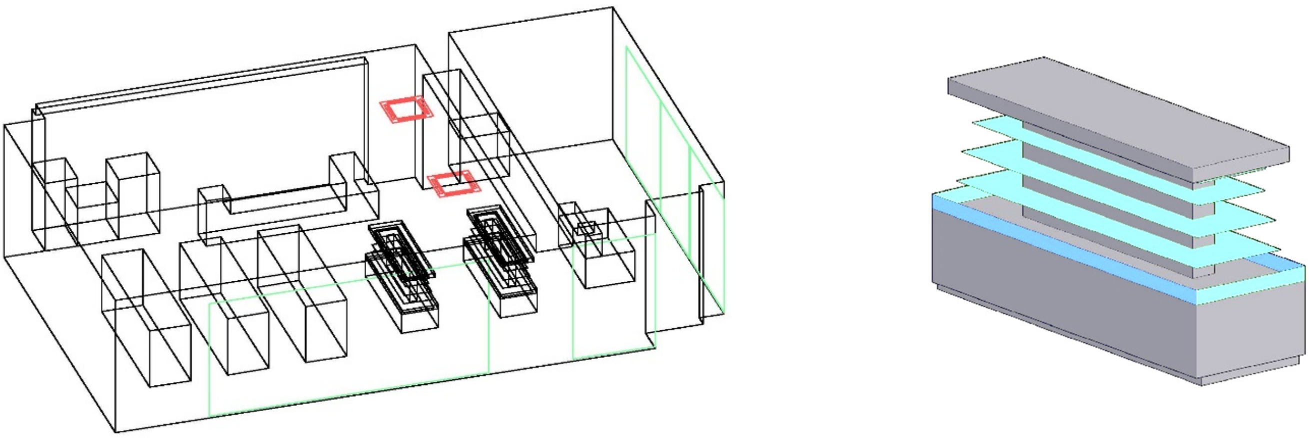

(**a**) (**b**)

Figure 3. Geometry model; (**a**) convenience store; (**b**) CSS.

In this study, four different setting temperature conditions were simulated, compared, and analyzed. The steady-state condition was used in the simulation setup with the realizable k-ε as the turbulence model. The boundary conditions for the CFD model were provided by the field measurement, such as air velocity from the AC system and different setting air temperatures, which can be seen in Table 2. The heat generated by walls, windows, and the door was assumed to be the convection heat transfer, which comes from the ambient temperature. For the internal wall, the free stream temperature was measured at 27 °C with the amount of heat transfer coefficient being 3.9 W/m^{2}K, respectively. Based on the simulation, basic assumptions for this study are divided into:

(1) 3 Dimensions with a coordinate system.
(2) The fluid is an incompressible flow.
(3) The inlet air velocity is evenly distributed.
(4) Not considering the buoyancy effects.
(5) Ignore viscous dissipation and radiation effects.

Table 2. Boundary conditions of the simulation.

Boundary Condition	Type	Value
Supply Air	Velocity Inlet	Velocity: 2.5 m/s Temperature: 14 °C
Return Air	Pressure Outlet	Temperature: 22 °C, 24 °C, 26 °C, 28 °C
Wall	Wall	Thermal condition: Convection Heat transfer coefficient: 3.9 W/m^{2}K Free stream temperature: 27 °C Wall thickness: 0.20 m
Total heat source	Wall	Heat flux: 150 W/m^2

As shown in Figure 4a, a number of grid tests were performed in this CFD simulation with varying temperature values within a five-point range. Temperature data can be depicted graphically by a variety of grids, as illustrated in Figure 4b, using comprehensive data. In addition, the relative error in the number of grids was calculated and shown in Table 3. To solve all of the equations concurrently, the well-known finite control volume approach using a Semi-Implicit Method for Linked Equations (SIMPLE) algorithm is used.

Since the numerical simulation method will focus on the temperature and air distribution, the number of grids is critical to affecting the calculation efficiency and accuracy for simulation. The average temperature in the convenience store is chosen to assess the right number of grids. Five sets of the number of grids are selected for comparison to verify the relative error (%) of the temperature under different numbers of grids. The relative error (%) can be determined by using the Equation (1). The average temperature grid test is shown in Table 3. The grid numbers start at 100,890 with a relative error value under 10% for each grid. However, while the number of grids increases from 773,384 to 912,790 with a relative error value of 2.59%, it reveals the temperature change is not so obvious. After compromising the simulation time and accuracy, this research will adopt the grid number of 1,124,035 for numerical simulation.

$$Relative\ Error\ (\%) = \left| \frac{Current\ Grid\ Error - Previous\ Grid\ Error}{Current\ Grid\ Error} \right| \quad (1)$$

Table 3. The relative error in the number of grids.

Number of Grids	Relative Error (%)				
	Point 1	Point 2	Point 3	Point 4	Point 5
100,890	Base	Base	Base	Base	Base
294,502	7.44	5.02	0.60	12.92	7.51
454,922	5.02	1.63	6.27	12.81	2.53
501,640	0.04	12.48	7.94	8.53	0.93
733,384	1.56	2.61	7.80	1.47	2.91
912,790	2.59	1.36	0.52	3.96	0.73
1,124,035	0.27	0.01	0.04	0.05	0.05

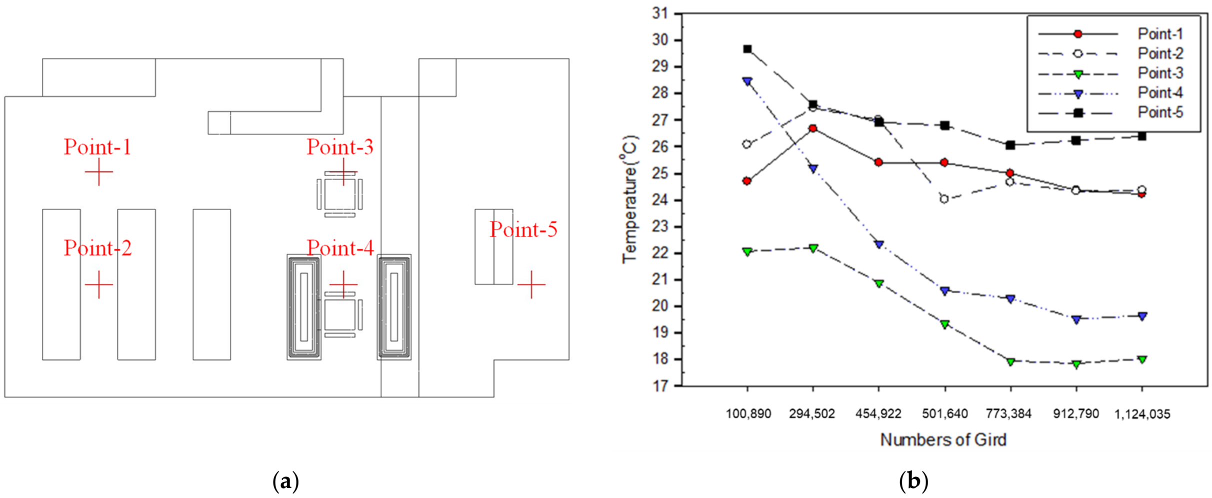

Figure 4. Grids test; (**a**) sample point location; (**b**) the number of grids.

5. Results and Discussion

5.1. Field Measurement

There is a relatively low-temperature phenomenon near the CSS. As illustrated in Figure 5, when the setting temperature of the AC is 26 °C, the temperature in the center of the middle aisle CSS is relatively low. The temperature measured from 120 cm away from the ground has an average temperature of 21.1 °C. At the same time, the average temperature is 17.6 °C at a distance of 80 cm from the ground. Then measured from 40 cm above the ground, the average temperature is 13.7 °C. This also proves that the low-temperature air-conditioning leaking from the open display cabinet will cause cold feet, which has a great influence on the ambient temperature.

After conducting the analysis based on energy consumption and the ambient temperature of the baseline energy usage intensity (EUI) of convenience stores could be derived from simulation data accordingly. Figure 6. shows the energy consumption for each AC under daily and monthly conditions. There is the highest power consumption in the daily and monthly conditions. The line graph illustrates the amount of two kinds of AC system locations (near the walkway and CSS) that consume power. Figure 6a shows power consumption increased over the time given for AC near the walkway, while AC near the CSS tends to be constant. It also shows that the highest daily energy consumption is around 14:00 for AC-1 near the walkway than AC-2 near the CSS, which shows stable condition. In addition, Figure 6b shows power consumption fluctuated over a month. Concerning the amount of power consumption used, it began at around 50 kW and then decreased at 30 kW, after which the figure fluctuated slightly until at 35 kWh for the AC-1 near the walkway. Likewise, approximately 20 kW power consumption of AC-2 near the CSS was used on the first day, after which the figure fluctuated slightly and on the final day to around 13 kW. Overall results, the AC-2 which is located near the CSS presents the lower power consumption. The CSS generates cold air, which could affect the surrounding environment cooler. It also affects the temperature set point in AC-2 near CSS, which often cuts in and cuts out the power. As a result, the AC sensor/thermostat detects that the environment has met the indoor requirements and takes action to reduce the load.

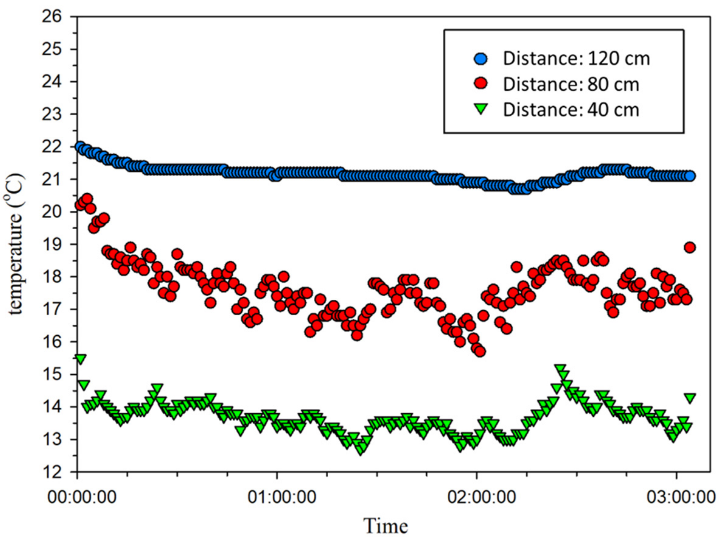

Figure 5. The measured temperature at the CSS middle aisle in the C-C′ section plane.

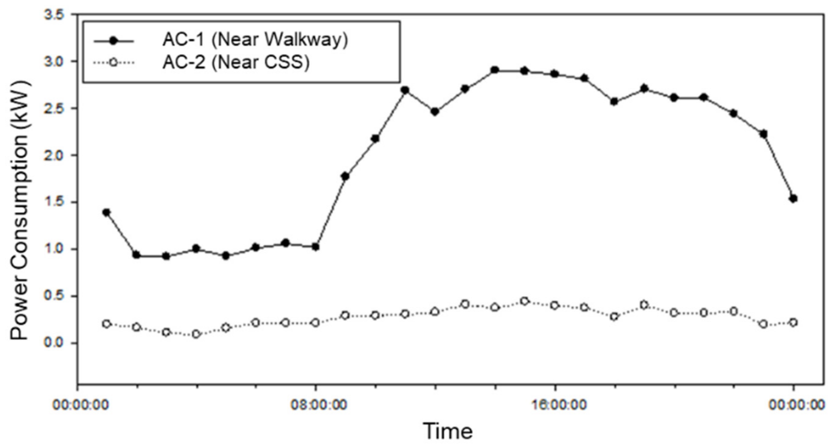

(**a**)

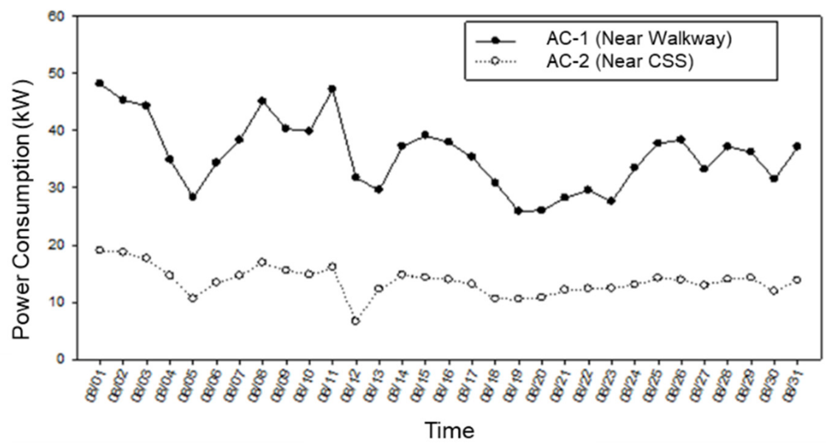

(**b**)

Figure 6. Power consumption of AC system; (**a**) 24-h; (**b**) monthly.

Illustrated in Figure 7 is the amount of annual power consumption for AC. Units are measured in kWh. It begins at more than 15,000 kWh in January and then decreases to around 15,216 kWh. The energy consumption increased until June at around 23,055 kWh. On the other hand, the power consumption of AC after June decreased slightly until around 15,000 kWh in December. Furthermore, the highest annual power consumption of AC was in June with an almost increased 23,055 kWh.

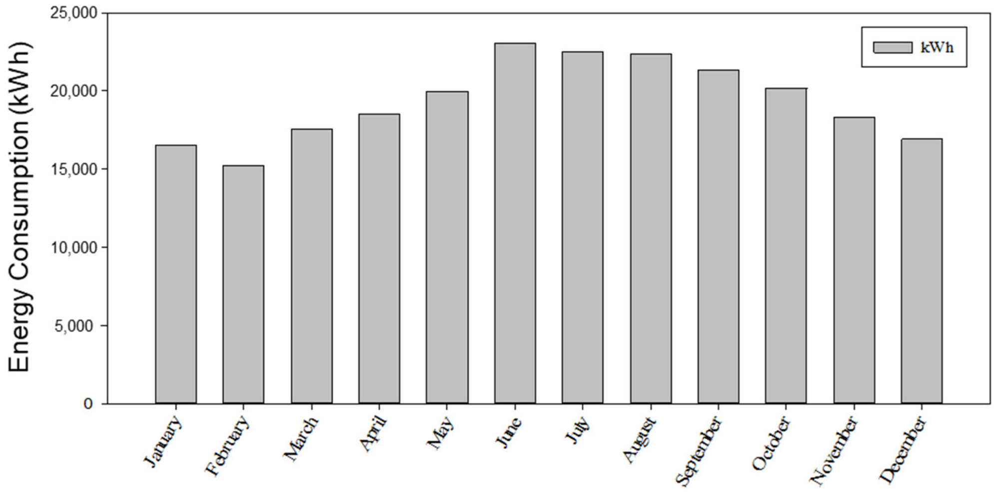

Figure 7. Annual energy consumption of AC.

5.2. CFD Simulation

The CFD approach was applied to evaluate the thermal environment conditions under different supply air temperatures in the convenience store. The air temperature model is solved using the four different CFD models. It can be seen that the velocity parameters could reach the desired temperature of 22 °C with a tolerance temperature of ±2 °C. The results at different set temperatures field are shown in Figure 8 which is located at the A-A′ section plane. The range temperature is from 5 °C to 30 °C. It can be found that the upper air temperature over the air AC forms a good protective cover. So that lower air temperature under the cover of the AC, the warm air from the warm food area at the upper right cannot effectively reach the desired temperature. Near the open-type CSS, the temperature increases to 22 °C. When the set temperature rises from 22 °C to 28 °C in the upper left of the room, the temperature increases significantly to 25 °C. Although there is a snack rack at the bottom left, allowing the leaking air of the CSS to form a backflow, the flow field is thrust upward the rack, and mixed with the cool air blown by the air conditioner to block the hot air in other areas. The setting is changed in the middle aisle of the CSS. The temperature change is more obvious, mainly due to the interaction of low air leakage from the CSS and AC, and the temperature rises from about 18 °C to 22 °C. In the actual environment, the operation of the AC will be affected by the temperature of the return air. After the simulation of the airflow velocity of the AC of 2.5 m/s, it is found that the return air temperature will be lower than each set temperature, and the air conditioner will operate at a reduced load, so this study further reduces the outlet airflow velocity of AC-2 and observes the impact on the environment and the CSS when the airflow velocity is lower.

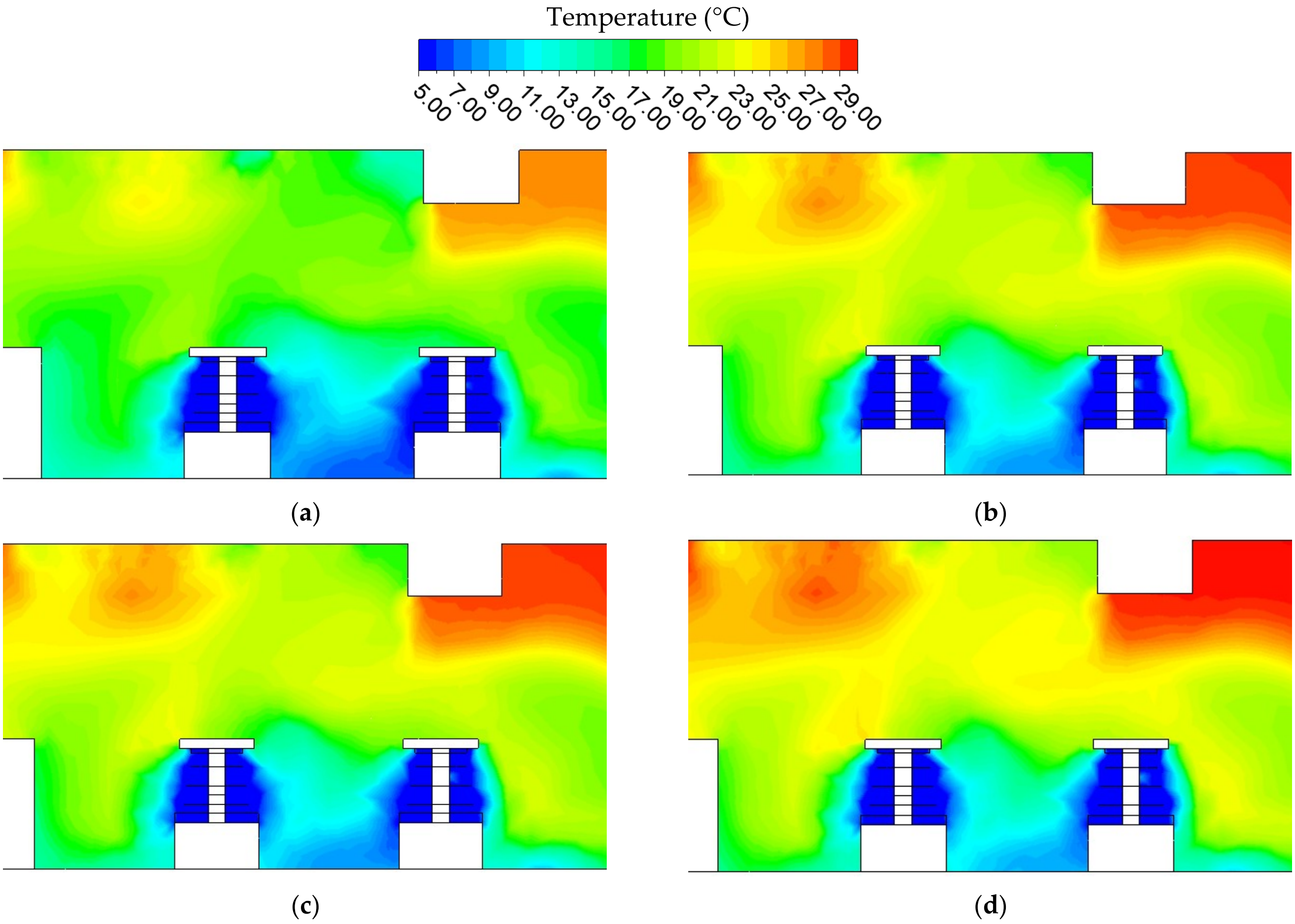

Figure 8. Temperature distributed profile at different thermostat set point (v = 2.5/s); (**a**) T = 22 °C; (**b**) T = 24 °C; (**c**) T = 26 °C; (**d**) T = 28 °C.

However, no matter what temperature the AC is set at, it can be found that the environment around the CSS is in a low-temperature state. When the environment is near the temperature set by the air conditioner, the temperature near the CSS can be lower than other the temperature is around 3–5 °C, which also means that the impact of the CSS on the surrounding environment is huge and cannot be ignored. Under the influence of this leaked low-temperature air. The return air temperature of the adjacent AC will drop. The sensor of the AC judges that the environment has reached the required indoor temperature and performs the action of reducing the load. After the load is reduced, it is easy for other hot air to intrude into the vicinity of the CSS. The cold air of the cabinet also cools the environment, which in turn increases the load on the CSS.

The airflow temperature between AC-1 and AC-2 was evaluated at different heights (from the floor to the ceiling) and also different temperature settings for each at 22 °C, 24 °C, 26 °C, and 28 °C, as shown in Figure 9. The different heights will produce different temperature results. When the air velocity is 2.5 m/s, the monitoring results of AC-1 are shown in Figure 9a. It can be found that when the set temperature is increased, the room temperature is also increased accordingly. When the height is raised from the floor to 1.8 m, it can be found that the temperature in this state is cooler, and then as the height rises, the temperature is also increasing. When the set temperature is 22 °C, the return air temperature is about 23.5 °C. When the set temperature increases, the temperature detected by the return air also increases. When the set temperature is 28 °C, the return air temperature is also about 28 °C.

In the middle of the CSS and the monitoring line of the AC-2, the temperature is shown in Figure 9b. It can be found that when the height is raised from the floor to about 1.8 m, the temperature gradually increases from low temperature. Then as the height rises, the phenomenon of the temperature becoming warm is not obvious, which means that in this area, there is no hot air absorbed from the outside or the air blocked by the beam backflow and balance each other. At the height of 1.2 m, the temperature of the air conditioner is set at 22 °C, while the temperature in the middle of the CSS is only about 14 °C. When the set temperature is raised to 28 °C, the temperature is only about 19 °C, which is significantly different from the operating temperature in other places. The ambient temperature in the middle of the CSS will be significantly affected by the leakage of low-temperature cold air.

The overall temperature from the height of 0 m to 1.8 m is relatively lower than at other heights, specifically near the AC-2, which is located in between the CSS. It revealed that the CSS produced the cold air around 8 °C to 10 °C. The situation would make the sensor of the AC-2 sense that the set temperature has been reached and also often occurred cut-off. Furthermore, the cold effect from the CSS could be used to take advantage by increasing the temperature set point of the AC-2 to produce energy-saving.

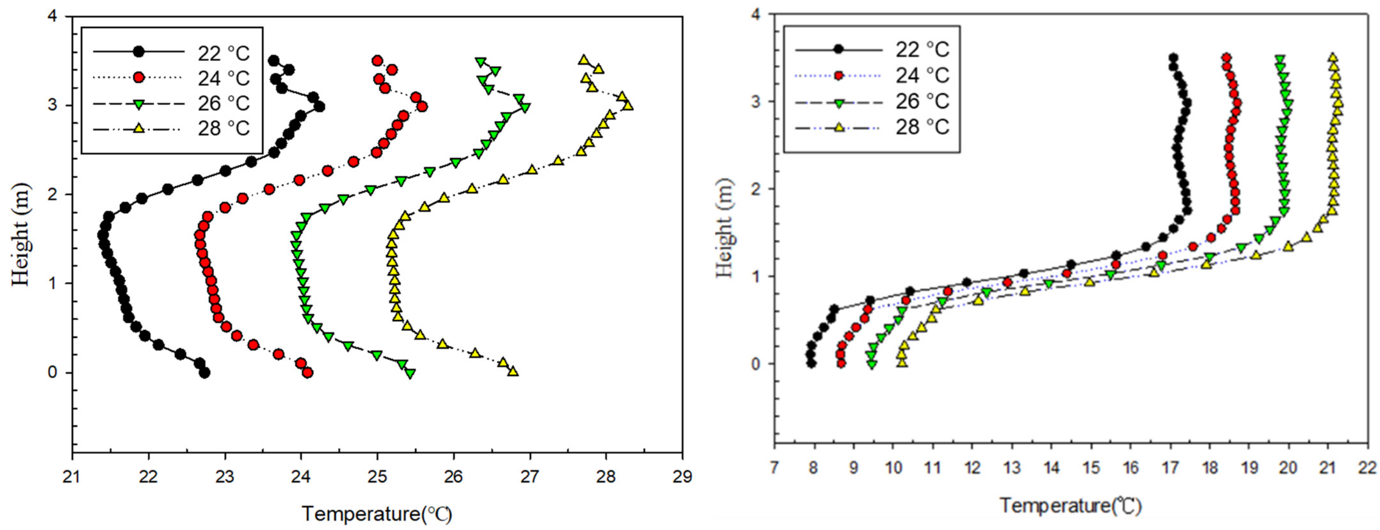

(**a**) (**b**)

Figure 9. Temperature in different heights; (**a**) AC-1 near walkway; (**b**) AC-2 near CSS.

6. Conclusions

This study takes a convenience store to conduct energy consumption measurement and CFD simulation analysis to study the impact of the environment on the CSS. From the energy consumption monitoring, it is found that the peak electricity consumption of the convenience store is June with 23,055 kWh, and the lowest electricity consumption is 15,216 kWh in February. Electricity is usually considered the most power-consuming. The AC consumes 14.73% of electricity. In terms of the power consumption of the AC, it was found that the power consumption of the two AC systems was uneven. Through CFD simulation, it is found that when the environment is near the temperature set by the AC, the temperature near the CSS can be 3–5 °C lower than in other places. Under the influence of low-temperature air effects from CSS, it will further cause the temperature of the return air of the adjacent AC drops. Therefore, the sensor of AC determines that the environment has reached the indoor requirements and performs the action of reducing the load. Then, it uses the low temperature from the CSS to cool the environment and increases the CSS power consumption. After changing the AC temperature setting, it is found that the AC cannot successfully reach the desired temperature. The air intrusion in the hot area increases the extra load of the CSS. Furthermore, the cold feet effect of the CSS might be exploited to its advantage by increasing the temperature set point of the AC-2 to achieve energy savings.

The convenience store's average energy usage intensity (EUI) was much greater than that of office buildings and hotels. The research related to the energy consumption in a convenience store with a small area, but high equipment density will produce higher EUI than other building applications. So, it is important to evaluate and maintain the condition of the convenience store in order could achieve a lower EUI and energy-efficient concern.

Author Contributions: Conceptualization, F.W. and K.; Data curation, C.L. and K.; Formal analysis, K. and W.C.; Investigation, F.W., K. and I.P.; Methodology, K., W.C., C.L. and I.P.; Validation, K. and I.P.; Visualization, I.P.; Writing—original draft, K. and C.L.; Writing review and editing, F.W. and I.P. All authors have read and agreed to the published version of the manuscript.

Funding: This research received no external funding.

Institutional Review Board Statement: Not applicable.

Informed Consent Statement: Not applicable.

Data Availability Statement: The data presented in this study are available on request from the corresponding author.

Conflicts of Interest: The authors declare no conflict of interest.

References

1. Kuo, C.F.J.; Lin, C.H.; Lee, M.H. Analyze the energy consumption characteristics and affecting factors of Taiwan's convenience stores-using the big data mining approach. *Energy Build.* **2018**, *168*, 120–136.
2. Kuo, P.Y.; Fu, J.C.; Jhuo, C.H. Analysis on the usage characteristics of electrical equipment of Taiwan's convenience stores. In Proceedings of the 2013 International Conference on Information Technology and Computer Application Engineering, Hongkong, China, 27–28 August 2013.
3. Wang, F.; Lin, H.; Tu, W.; Wang, Y.; Huang, Y. Energy modeling and chillers sizing of HVAC system for a hotel building. *Procedia Eng.* **2015**, *121*, 1812–1818. [CrossRef]
4. Wang, A.P.; Hsu, P.L. The network-based energy management system for convenience stores. *Energy Build.* **2008**, *40*, 1437–1445. [CrossRef]
5. Chou, D.C.; Chang, C.S.; Hsu, Y.Z. Investigation and analysis of power consumption in convenience stores in Taiwan. *Energy Build.* **2016**, *133*, 670–687. [CrossRef]
6. Litardo, J.; Hidalgo-Leon, R.; Soriano, G. Energy Performance and Benchmarking for University Classrooms in Hot and Humid Climates. *Energies* **2021**, *14*, 7013. [CrossRef]
7. Sadowska, B.; Piotrowska-Woroniak, J.; Woroniak, G.; Sarosiek, W. Energy and Economic Efficiency of the Thermomodernization of an Educational Building and Reduction of Pollutant Emissions—A Case Study. *Energies* **2022**, *15*, 2886. [CrossRef]
8. Sleiti, A.K.; Al-Ammari, W.A.; Al-Khawaja, M. Review of innovative approaches of thermo-mechanical refrigeration systems using low grade heat. *Int. J. Energy Res.* **2020**, *44*, 9808–9838. [CrossRef]
9. Borikar, S.A.; Gupta, M.M.; Alazawi, M.A.; Malwe, P.D.; Moustafa, E.B.; Panchal, H.; Elsheikh, A. A Case Study on Experimental and Statistical Analysis of Energy Consumption of Domestic Refrigerator. *Case Stud. Therm. Eng.* **2021**, *28*, 101636. [CrossRef]
10. ENERGY STAR, ENERGY STAR Buildings and Plants. ENERGY STAR Certification for Buildings. Available online: https://www.energystar.gov/buildings/building_recognition/building_certification (accessed on 15 March 2022).
11. Nikolaou, T.; Kolokotsa, D.; Stavrakakis, G. Review on methodologies for energy benchmarking, rating and classification of buildings. *Adv. Build. Energy Res.* **2011**, *5*, 53–70. [CrossRef]
12. Wang, F.; Lin, H.; Luo, J. Energy Consumption Analysis with a Weighted Energy Index for a Hotel Building. *Procedia Eng.* **2017**, *205*, 1952–1958. [CrossRef]
13. Lee, D.; Cheng, C.C. Energy savings by energy management systems: A review. *Renew. Sustain. Energy Rev.* **2016**, *56*, 760–777. [CrossRef]
14. Wang, X.; Dennis, M.; Jiang, J.; Zhou, L.; Zhai, X.; Lipiński, W. Performance of a novel cold thermal storage material in an emulated air conditioning system using different storage strategies. *Int. J. Refrig.* **2019**, *104*, 259–269. [CrossRef]
15. Yang, J.; Dong, Z.; Yang, H.; Liu, Y.; Wang, Y.; Chen, F.; Chen, H. Numerical and Experimental Study on Thermal Comfort of Human Body by Split-Fiber Air Conditioner. *Energies* **2022**, *15*, 3755. [CrossRef]
16. Aryal, P.; Leephakpreeda, T. CFD Analysis on Thermal Comfort and Energy Consumption Effected by Partitions in Air-Conditioned Building. *Energy Procedia* **2015**, *79*, 183–188. [CrossRef]
17. Jeon, B.K.; Kim, E.J. White-Model Predictive Control for Balancing Energy Savings and Thermal Comfort. *Energies* **2022**, *15*, 2345. [CrossRef]
18. Borgstein, E.H.; Lamberts, R.; Hensen, J.L.M. Evaluating energy performance in non-domestic buildings: A review. *Energy Build.* **2016**, *128*, 734–755. [CrossRef]

19. Chen, Z.; Xin, J.; Liu, P. Air quality and thermal comfort analysis of kitchen environment with CFD simulation and experimental calibration. *Build. Environ.* **2020**, *172*, 106691. [CrossRef]
20. Luzi, G.; McHardy, C. Modeling and Simulation of Photobioreactors with Computational Fluid Dynamics—A Comprehensive Review. *Energies* **2022**, *15*, 3966. [CrossRef]
21. Sakiyama, N.R.M.; Frick, J.; Bejat, T.; Garrecht, H. Using CFD to Evaluate Natural Ventilation through a 3D Parametric Modeling Approach. *Energies* **2021**, *14*, 2197. [CrossRef]
22. Bhamjee, M.; Nurick, A.; Madyira, D.M. An experimentally validated mathematical and CFD model of a supply air window: Forced and natural flow. *Energy Build.* **2013**, *57*, 289–301. [CrossRef]
23. Shan, X.; Xu, W.; Lee, Y.K.; Lu, W.Z. Evaluation of thermal environment by coupling CFD analysis and wireless-sensor measurements of a full-scale room with cooling system. *Sustain. Cities Soc.* **2019**, *45*, 395–405. [CrossRef]
24. Papakonstantinou, K.; Chaloulakou, A.; Duci, A.; Vlachakis, N.; Markatos, N. Air quality in an underground garage: Computational and experimental investigation of ventilation effectiveness. *Energy Build.* **2003**, *35*, 933–940. [CrossRef]
25. Catalina, T.; Virgone, J.; Kuznik, F. Evaluation of thermal comfort using combined CFD and experimentation study in a test room equipped with a cooling ceiling. *Build. Environ.* **2009**, *44*, 1740–1750. [CrossRef]
26. Huang, K.; Song, J.; Feng, G.; Chang, Q.; Jiang, B.; Wang, J.; Sun, W.; Li, H.; Wang, J.; Fang, X. Indoor air quality analysis of residential buildings in northeast China based on field measurements and longtime monitoring. *Build. Environ.* **2018**, *144*, 171–183. [CrossRef]
27. Zhang, Z.; Chong, A.; Pan, Y.; Zhang, C.; Lam, K.P. Whole building energy model for HVAC optimal control: A practical framework based on deep reinforcement learning. *Energy Build.* **2019**, *199*, 472–490. [CrossRef]
28. Song, J.; Meng, X. The improvement of ventilation design in school buildings using CFD simulation. *Procedia Eng.* **2015**, *121*, 1475–1481. [CrossRef]
29. Cheng, C.C.; Lee, D. Smart sensors enable smart air conditioning control. *Sensors* **2014**, *14*, 11179–11203. [CrossRef]
30. ANSYS Fluent, Workbench 2020 R2. Available online: https://www.scribd.com/document/478910198/ANSYS-FluentTutorial-Guide-2020-R2-pdf (accessed on 6 March 2021).